

1 **Non-targeted multimodal metabolomics and lipidomics data from ovine rumen fluid**
2 **fractions**

3 Nikola Palevich^{1*}, Paul H. Maclean¹, Arvind K. Subbaraj² and Mingshu Cao¹.

4 ¹AgResearch Ltd., Grasslands Research Centre, Palmerston North, 4442, New Zealand.

5 ²AgResearch Ltd., Lincoln Research Centre, Christchurch, 7674, New Zealand.

6 *Corresponding author: E-mail: nik.palevich@agresearch.co.nz

7 **Keywords**

8 Metabolomics, Lipidomics, Ovine, Rumen fluid.

9 **Abstract (250 words maximum)**

10 **Background:** Metabolomics is a powerful and sensitive approach for investigating low molecular weight
11 metabolite profiles present in rumen biofluids to identify potential roles of metabolites in rumen microbiome
12 and understanding host-level regulatory mechanisms associated with animal production.

13 **Findings:** Rumen samples from sheep grazed on a mixed ryegrass and clover pasture diet, were fractionated
14 based on molecular weight and analysed using metabolomics and lipidomics to detect the small molecules
15 present in ovine rumen fluid fractions.

16 **Conclusions:** Untargeted metabolomics provides a detailed snapshot of the ovine ruminal fluid metabolome
17 that can be used as reference for future studies on ovine rumen fluid or as a comparator for other ruminant
18 species. All data and metadata are available for download in the MetaboLights database.

19 **Data description**

20 Ruminant livestock are an important component of feeding the growing human population while also being
21 sources of global greenhouse gas emissions. Rumen microbiota breakdown and convert plant polysaccharides
22 from feed into energy sources but also result in methane formation that affect ruminant productivity. As such,
23 characterisation of the low molecular weight metabolites is key to improving our understanding of the rumen
24 metabolome and our pursuit of developing a system-wide picture of rumen metabolism and biology.

25 Metabolomics facilitates our ability to rapidly detect hundreds to thousands of metabolites within a single
26 sample and enables accurate measurement of end-products of complex, genetic, epigenetic and environmental
27 interactions. While rapid developments in genomics have accelerated our knowledge of rumen biology at the
28 molecular level [1-8], there has been less work focusing on the low molecular weight molecules that stem
29 from rumen fermentation of feed, and a complete absence of metabolomics studies on ovine rumen samples
30 [9-11]. To date, only the bovine rumen fluid has been characterised using metabolomics [12-17].

31 Moreover, past studies on the rumen metabolome have used a ‘freeze dry/grind/extract/inject’ approach, which
32 ignores the highly biodiverse ecology that is the rumen, with bacteria, fungi, higher order microbes, plant
33 material at different stages of breakdown, all encased in a mammalian environment. As such, there is a need
34 to address these major research and literature gaps as it is the rumen microbial communities that underlie
35 variations in undesirable methane formation and conversion of feed to useful animal products. The presented
36 dataset was initially collected to study the metabolic signatures of the ovine rumen with the purpose of
37 increasing rumen digestibility of various forages and enhancing animal performance. However, significant
38 challenges exist for analysing ruminal biochemistry and identifying metabolites within the chemically
39 complex and heterogenous rumen fluid that have been shown to vary greatly based on dietary factors and host
40 species [1, 10]. Also, an important consideration for metabolome studies is the impact of sample collection
41 prior to extraction.

42 As such, we performed an analysis of the rumen metabolome using a newly developed *in vitro* system, using
43 different molecular weight cut-off points that represent different fractions of the rumen *in vitro* and could lead
44 to better understanding of how different components of the rumen interact. Studies were conducted with an *in*
45 *vitro* simulation of the rumen fermentation using a simple *in vitro* artificial rumen system of permeable

46 continuous culture type which would simulate both the removal of end-products of fermentation and flow of
47 ingesta. Experiments were made to determine the effects of dialysis on the fermentation and microbial
48 population in the continuous culture. In addition we accounted for the macro components of rumen fluid such
49 as large degraded plant material associated with the digestion of common fibrous feeds or associated microbial
50 features and proteins, by obtaining filtrates from dialysis of rumen fluid through membranes with molecular
51 weight cut-offs of 20 kDa, 8-10 kDa and 100 Da. These three fractions are expected to exclude large tannin-
52 rich plants extracts and proteins respectively. We then performed metabolomic profiling of the enriched low
53 molecular weight dialyzed rumen fluid (DRF) fractions to investigate biologically relevant molecules such as
54 phenolics, phospholipids, amino acids, dicarboxylic acids, fatty acids, volatile fatty acids, glycerides,
55 carbohydrates and cholesterol esters. In this study, an untargeted approach using multimodal methodologies
56 including polar and semi-polar-retention chromatographies coupled to mass spectrometry, have been used to
57 detect a wide-range of metabolites encompassing polar, semi-polar compounds and lipid species. A basic
58 overview of the datasets and experimental design is shown in Figure 1.

59 Sample collection

60 Whole rumen content samples were collected post-mortem and pooled from five sheep grazing *ad libitum* on
61 a ryegrass and clover pasture diet. Approximately 5 L of rumen contents were collected from each animal and
62 filtered through 4 layers of cheesecloth (335 μ m mesh) to remove plant material present in the digesta (Figure
63 1A). The pH of each sample was determined immediately after sampling using a pH meter (6.6). Filtered
64 rumen fluid was immediately processed so as not to alter the fermentative capacity of the ruminal fluid.
65 Sampling was conducted in December 2018 at AgResearch Grasslands Research Centre (Palmerston North,
66 New Zealand) under the approval of the AgResearch Grasslands Animal Ethics Committee.

67 A method was developed to acquire DRF fractions that enrich for different sized components of rumen fluid
68 for metabolomics and lipidomics analyses (Figure 1B). DRF fractions based on three molecular weight cut-
69 offs (MWCO) were obtained using Spectra-Por® Float-A-Lyzer® G2 dialysis systems with MWCOs of 20
70 kDa (Z726931, Sigma-Aldrich), 8-10 kDa (Z726605, Sigma-Aldrich) and 100 Da (Z727253, Sigma-Aldrich).
71 Briefly, the pooled and filtered RF contents were mixed and divided evenly into four Schott gas washing
72 bottles fitted with Drechsel type head connections (GL 14, DURAN). The analytical conditions *in vitro* were

73 identical to the animal's physiological conditions, with a temperature of 39°C in anaerobic conditions obtained
74 by insufflating a stream of O₂-free CO₂ inside the container with constant mixing. To obtain each DRF
75 fraction, five replicates of each individual MWCO apparatus were dialyzed against 10mL of autoclaved
76 phosphate buffered saline (1× PBS, 137 mM NaCl, 2.7 mM KCl, 8 mM Na₂HPO₄, and 2 mM KH₂PO₄, pH
77 7.4) buffer overnight at 39°C in a water bath. Additional containers were prepared in parallel containing only
78 PBS and distilled water as control treatments. The principles of dialysis allowed small compounds to migrate
79 from high concentration (rumen fluid contents) to low concentration (dialysis systems containing saline). DRF
80 fractions and samples of digesta obtained from different phases of the process were snap-frozen in liquid
81 nitrogen and kept on dry ice until long term storage at -80°C.

82 **Extractions for non-targeted metabolomic and lipidomic profiling**

83 A combination of multiple metabolomics platforms, or 'multi-modal' strategy, were applied in parallel to the
84 same batch of biological samples to facilitate interpretation and provide extensive coverage of the rumen
85 metabolome. To comprehensively elucidate metabolites associated with DRF fractions we used: hydrophilic
86 interaction liquid chromatography (HILIC) to separate polar compounds [18], ultra-high-performance liquid
87 chromatography (UHPLC) with C18 chromatography to separate semi-polar compounds and a modified C18
88 phase (CSH-C18) for separation of lipids [19-20]. LC-MS analyses were done in both positive and negative
89 electrospray ionization (ESI) modes.

90 Upon collection, the DRF fractions were snap-frozen in liquid nitrogen, transferred to glass vials and stored
91 at -80°C until further use. Seven aliquots of 1 mL each (5 for analyses and two for quality control samples
92 (QC)) of each sample were transferred into microcentrifuge tubes. The two QC samples (12) were pooled and
93 solely used for monitoring sample degradation, tracking run-order effects within a batch, and quality control
94 purposes only. Briefly, samples were thawed overnight at 4°C, centrifuged (4°C, 11,000 × g) for 10 min and
95 200 µL of supernatant transferred into a 2 mL micro-centrifuge tube. An extraction solvent comprising 800
96 µL of chloroform:methanol (1:1; v/v) was added and samples were vortexed (1 min). Sample was diluted with
97 water (400 µL), again vortexed (1 min), and centrifuged (4°C, 11,000 × g) for 15 min.

98 To evaluate the lipidome of the DRF fractions, the lower, organic layer was taken (200 µL), evaporated to
99 dryness under a continuous stream of nitrogen (30°C), and the dried extract was reconstituted in 200 µL of

100 chloroform:methanol (2:1; v/v), with 16:0 d₃₁-18:1 phosphatidylethanolamine (10 µg/mL) as an internal
101 standard. Finally, samples were vortexed (1 min), and 100 µL was transferred to a glass insert in an auto-
102 sampler vial for LC-MS analysis. For polar and semi-polar compounds, hydrophilic interaction liquid
103 chromatography (HILIC) and C18 chromatography were applied, respectively [18-20]. For these analyses,
104 supernatants (200 µL) were mixed with 800 µL of pre-chilled chloroform:methanol (1:1, v/v) containing 1.6
105 mg/L of internal standards; d5-Ltryptophan, d4-citric acid, d10-leucine, d2-tyrosine, d35-stearic acid, d5-
106 benzoic acid, 13C2-glucose, and d7-alanine. Two aliquots of the upper aqueous layer (200 µL) was taken and
107 evaporated as above, then reconstituted in 200 µL of the extraction solvents (acetonitrile:water containing
108 0.1% formic acid;1:1 for HILIC and 1:9 for C18, v/v).

109 **Chromatography and mass spectrometry spectral acquisition**

110 The chromatographic gradient and other conditions were selected to detect metabolites over a wide polarity
111 range for the non-targeted LC-MS and lipid analyses as previously described [18-20]. For semi-polar
112 compounds, C18 conditions were set as described [18], with extract (2 µL) injected into a 100 mm × 2.1 mm
113 Thermo Hypersil Gold C18 column with 1.9 µm particle size and eluted over a 16 min gradient with a flow
114 rate of 400 µL/min. The mobile phase was a mixture of water with 0.1% formic acid (solvent A), and
115 acetonitrile with 0.1% formic acid (solvent B). Chromatographic gradient and other LC-MS conditions have
116 been previously described [20-21]. For polar compounds, HILIC conditions were set as described [18], with
117 extract (2 µL) injected onto a 100 mm × 2.1 mm ZIC-pHILIC column with 5 µm particle size and eluted over
118 17 min with solvent gradient from 97% solvent A (1 min), 97%-70% solvent A (1-12 min), 70-10% solvent
119 A (12-14.5 min) to 10% solvent A (14.5-17 min). Mobile phase solvent A was a mixture of acetonitrile with
120 0.1% formic acid, solvent B was a mixture of water with 16 mM ammonium formate and flowrate was 250
121 µL/min. Chromatographic gradient and other LC-MS conditions have been previously described [18, 22].

122
123 C18 and HILIC column effluents were connected to a high-resolution mass spectrometer (Exactive
124 Orbitrap™, ThermoFisher Scientific, Waltham, MA, USA) mass spectrometer with electrospray ionization,
125 and lipid analysis was conducted on a Q-Exactive quadrupole-high resolution mass spectrometer
126 (ThermoFisher Scientific, Waltham, MA, USA). Both full and data dependent MS² (ddMS²) scans were

127 collected in profile data acquisition mode. For full scan mode, a mass resolution setting of 35,000 was set to
128 record a mass range of m/z 200-2000 with a maximum trap fill time of 250 ms. In ddMS², MS² measurements
129 are activated when a set peak intensity threshold is achieved. For ddMS² scan mode, the same mass resolution
130 setting was maintained with a maximum trap fill time of 120 ms. The isolation window of selected MS¹ scans
131 was \pm 1.5 m/z with a normalized collision energy of 30. Samples were run in both positive and negative
132 ionization modes separately. Positive ion mode parameters were as follows: spray voltage, 4.0 kV; capillary
133 temperature, 275 °C; capillary voltage, 90 V; tube lens 120 V. Negative ion mode parameters were as follows:
134 spray voltage, -2.5 kV; capillary temperature, 275 °C; capillary voltage, -90 V; tube lens, -100 V. The nitrogen
135 source gas desolvation settings were the same for both modes (arbitrary units): sheath gas, 40; auxiliary gas,
136 10; sweep gas, 5.

137 Pooled sample from all conditioned DRF fraction extracts and internal standards were used as controls and
138 samples were run in randomised order to avoid bias due to any inherent variation due to run order. Blank
139 subtraction was applied after internal standard correction. To verify and maintain data quality, the QC sample
140 was injected once every 10 samples. Retention time, signal intensity, and mass error of the internal standard
141 were constantly monitored during the runs. Fragmentation data on approximately 4 samples in total per
142 ionization mode (positive and negative) were used for identification of metabolite ions/classes.

143 **Data quality, processing and analysis**

144 The MS raw data files (Thermo .raw files) were converted to mzXML files using MSConvert function of
145 ProteoWizard™ [23]. These files were uploaded to XCMS Online [24, 25] with suitable parameters for data
146 processing including peak detection, retention time alignment, profile alignment, isotope annotation, grouping
147 and gap filling. The type of adducts generated are dependent on the solvents and eluting conditions used. For
148 this study, [M+H] and [M+NH₄] adducts were selected for negative and positive ionisation modes,
149 respectively. Finally, a retention time tolerance of 0.1 min, and mass error tolerance of \pm 10 ppm was allowed.
150 The filtered matrix was normalized by a QC based on LOESS signal correction (QC-RLSC) [26] and all
151 subsequent m/z features and retention times with relative standard deviation (RSD) [27] $>$ 0.3 were eliminated.
152 The resultant data matrix was used for downstream statistical analyses and metabolite identification.

153 Statistical analysis and metabolite annotation/identification

154 Following the metabolomics data analysis pipeline [28] the raw data from the lipid stream (Figure 1C) were
155 processed and subjected to peak detection, quality control, statistical analysis, and the annotation of the top-
156 ranking peaks. Metabolite features were initially confirmed by matching source-induced fragmentation data
157 against standard MS/MS spectra in the METLIN MS² spectral library using [XCMS Online](#) [24, 25]. The fold
158 change (FC ≥ 2), *p*-value (*p* < 0.1), and intensity thresholds (10,000) were defined for peak ranking. The
159 identity of significantly differential peaks were further determined from the exact mass composition using
160 HMDB [29], LIPID MAPS [30], METLIN [31], LMDB [9], BMDB [32], [PubChem](#) and [mzCloud](#) databases.
161 All the raw data and metadata reported in this study have been submitted to the MetaboLights database
162 (www.ebi.ac.uk/metabolights) with the study identifier: [MTBLS1717](#).

163 Because only sparse fragmentation spectra (MS²) were collected for positive mode ions and no MS² for
164 negative mode ions in this study we used the correlation structure of peaks for metabolite identification. Unless
165 otherwise specified, we carried out MSI (Metabolomics Standards Initiative) level 2 metabolite annotation as
166 evidenced by chromatographic behaviour, library search based on accurate mass (< 10 ppm error) and the
167 match of isotopic peak intensity between experimental and theoretical spectrum. For peaks detected with C18
168 and HILIC chromatography, after the filtering of ¹³C isotopic peaks and early eluting peaks (<1 min) were left
169 for annotation in each ionization stream. Metabolite identification was based on the match of *m/z* ([M+H],
170 [M+NH₄] or [M-H], within 5 ppm accuracy) with those in HMDB and in-house retention time databases. In
171 addition, we exploited the correlation structure of top peaks to assist the annotation. Correlated peaks due to
172 coelution may indicate the similar physio-chemical properties of eluting metabolites, or in-source fragment
173 ions [28]. The presence of in-source fragment peaks helps identify the molecular ion for correct annotation of
174 the metabolite. On the other hand, peak correlation among biological samples may suggest the origin of
175 candidate metabolites, providing additional information for annotation.

176 For identifying significant peaks (FDR corrected *p* value ≤ 0.05 , FC ≥ 1) as potential ovine rumen fluid
177 metabolome products, a multi-group comparison between the DRF fractions (20 kDa, 8-10 kDa, 100 Da)
178 groups was performed (Figure 2). An initial prerequisite for our downstream comparative multimodal analyses
179 was that a peak needed to be present in ≥ 3 of the 5 biological replicates across each of the metabolomics

180 analysis. Univariate hypothesis testing of the peaks was carried out using Permutation ANOVAs as
181 implemented in the lmPerm R package version 2.1 [33] with 1 million permutations, after which, significance
182 was determined for the peaks using the Benjamini-Hochberg FDR-corrected [34] *p*-values (FDR *p* value <
183 0.05). A total of 675 peaks for HILIC, 144 C18 peaks and 454 peaks for LIPID were identified (both positive
184 and negative modes), with putative annotations were quantified with varying degree of confidence. Overall, a
185 combined total of 1,454 peaks were identified with no putative annotations across all metabolomics analyses.
186 This suggests that further correlation between metabolomics and transcriptomics data to aid in identifying
187 these unknown features is required and is an area of active research.

188 **Potential use**

189 To date, the majority of published ruminant metabolomics work has focused on the processed bovine ruminal
190 fluid metabolome [14-17]. This suggests that greater consideration needs to be given to what components are
191 extracted for understanding the rumen, as otherwise we may be mainly extracting the degraded pasture
192 metabolome that is destined for return to the pasture, rather than what is available for uptake by the ruminant.
193 Our data provides the first view of the ovine rumen metabolome during *in vitro* continuous culture using
194 multimodal metabolomics. Separating out these components has important implications for both animal
195 production, health assessment, disease diagnosis, bioproduct characterization and biomarker discovery for
196 desirable economic traits (e.g. feed efficiency and milk production). In particular, this dataset will serve as a
197 valuable resource in greenhouse gas research for future mining of targets for interventions that target the
198 rumen, including the search for potential vaccine candidates for methane mitigation strategies.

199 Future studies can employ various comprehensive bioinformatics tools to mine the presented raw data for any
200 metabolites that may be present in the ovine rumen, rather than focus solely on the top list of peaks. Also,
201 future efforts can employ more updated and curated databases such as BMDB [32] where Bovine rumen
202 metabolites and spectral data are archived. In addition, data can also be compiled for the other common
203 livestock species namely goats, horses and pigs, to compose an open access, comprehensive livestock
204 metabolome database focused on extremely low molecular weight metabolites. When coupled with the advent
205 of sequencing technologies and availability of genomic and transcriptomic datasets, is a comprehensive

206 approach for the identification of these peaks and characterization of the ovine rumen fluid molecular
207 mechanisms.

208 Different molecular weight cut-offs to separate out different components of the rumen led to different
209 metabolite and lipid profiles. While this finding is not surprising, it does suggest that fractionating rumen fluid
210 prior to extraction and analysis could give insights into metabolic activity occurring in relation to the solid
211 residue present compared to the more active liquid matrix. Biologically this may be due to the effects of
212 dialysis on fermentation patterns and subsequent shifts in microbial population during continuous culture. For
213 example, accumulation of particular fermentation end-products and variations in the composition of volatile
214 fatty acids (VFAs) can rapidly inhibit microbial growth within the rumen. Further work is needed to establish
215 whether higher molecular weight fractions can provide insight into the degree of breakdown of plant material.

216 This study is the first report of the ovine rumen metabolome, and while due to the collection method used is
217 not directly comparable to previously published bovine rumen metabolomes, represents an important reference
218 dataset. Our dataset should enable microbiologists and livestock researchers to conduct more targeted
219 metabolomic studies to identify low molecular weight features where further metabolome coverage is
220 required. Further research will be done on this prototype model, including additional data mining and
221 annotation of the metabolite features and investigation into the microbial community profiles within the
222 different dialysis contents using next-generation sequencing technology, as these microbiome signatures may
223 have critical implications into various livestock metabolomics applications.

224 **Availability of supporting data and materials**

225 Supporting data and corresponding metadata are available in the MetaboLights database [[MTBLS1717](#)].

226 **Abbreviations**

227 *m/z*: Mass-to-charge ratio; MS: Mass spectrometry; DRF: Dialyzed rumen fluid; MWCO: Molecular weight
228 cut-offs.

229 **Competing interests**

230 The authors declare that the research was conducted in the absence of any commercial or financial
231 relationships that could be construed as a potential conflict of interest.

232 **Authors' contributions**

233 NP conceived the project, designed and conducted all experiments, analyzed and interpreted the data, and
234 wrote the manuscript. PHM provided statistical and bioinformatics support for the project. AKS and MC
235 provided guidance with metabolomics and lipidomics analysis. All authors critically revised and approved the
236 final manuscript.

237 **Acknowledgments**

238 Special thanks to Linley Schofield in the Rumen Microbiology lab for providing the dialysis equipment. We
239 thank Hailey Gillespie and Trevor Holloway for their timely assistance with the collection of rumen fluid for
240 this study. We thank Alastair Ross and Karl Fraser for their revisions on the manuscript. This work was
241 supported by the AgResearch Ltd Strategic Science Investment Fund (SSIF, Grant No. C10X1702) to NP.
242 This work was also supported in part by the Agricultural and Marketing Research and Development Trust
243 (AGMARDT) Postdoctoral Fellowship Programme (Grant No. P17001) to NP.

244

References

245

1. Henderson G, Cox F, Ganesh S, Jonker A, Young W, Collaborators GRC, et al. Rumen microbial community composition varies with diet and host, but a core microbiome is found across a wide geographical range. *Scientific reports*. 2015;5 14567:1-13.
2. Seshadri R, Leahy SC, Attwood GT, Teh KH, Lambie SC, Cookson AL, et al. Cultivation and sequencing of rumen microbiome members from the Hungate1000 Collection. *Nature Biotechnology*. 2018;36 4:359-67.
3. Nayfach S, Roux S, Seshadri R, Udwary D, Varghese N, Schulz F, et al. A genomic catalog of Earth's microbiomes. *Nature Biotechnology*. 2021;39 4:499-509.
4. Borges DGL, Echeverria JT, de Oliveira TL, Heckler RP, de Freitas MG, Damasceno-Junior GA, et al. Discovery of potential ovicidal natural products using metabolomics. *PLOS ONE*. 2019;14 1:e0211237.
5. Palevich N, Kelly WJ, Leahy SC, Altermann E, Rakonjac J and Attwood GT. The complete genome sequence of the rumen bacterium *Butyrivibrio hungatei* MB2003. *Standards in Genomic Sciences*. 2017;12 1:72.
6. Palevich N, Kelly WJ, Ganesh S, Rakonjac J and Attwood GT. *Butyrivibrio hungatei* MB2003 competes effectively for soluble sugars released by *Butyrivibrio proteoclasticus* B316^T during growth on xylan or pectin. *Applied and Environmental Microbiology*. 2019;85 3:e02056-18.
7. Palevich N, Kelly WJ, Leahy SC, Denman S, Altermann E, Rakonjac J, et al. Comparative genomics of rumen *Butyrivibrio* spp. uncovers a continuum of polysaccharide-degrading capabilities. *Applied and environmental microbiology*. 2019;86 1.
8. Palevich N, Maclean PH, Kelly WJ, Leahy SC, Rakonjac J and Attwood GT. Complete genome sequence of the polysaccharide-degrading rumen bacterium *Pseudobutyrivibrio xylanivorans* MA3014 reveals an incomplete glycolytic pathway. *Genome Biology and Evolution*. 2020;12 9:1566-72.
9. Goldansaz SA, Guo AC, Sajed T, Steele MA, Plastow GS and Wishart DS. Livestock metabolomics and the livestock metabolome: A systematic review. *PLOS ONE*. 2017;12 5:e0177675.

269 10. Huws SA, Creevey CJ, Oyama LB, Mizrahi I, Denman SE, Popova M, et al. Addressing global ruminant
270 agricultural challenges through understanding the rumen microbiome: past, present, and future. *Frontiers*
271 in microbiology. 2018;9:2161.

272 11. Mao SY, Huo WJ and Zhu WY. Microbiome-metabolome analysis reveals unhealthy alterations in the
273 composition and metabolism of ruminal microbiota with increasing dietary grain in a goat model.
274 *Environmental Microbiology*. 2016;18 2:525-41.

275 12. Saleem F, Ametaj B, Bouatra S, Mandal R, Zebeli Q, Dunn S, et al. A metabolomics approach to uncover
276 the effects of grain diets on rumen health in dairy cows. *Journal of Dairy Science*. 2012;95 11:6606-23.

277 13. Li H, Yu Q, Li T, Shao L, Su M, Zhou H, et al. Rumen microbiome and metabolome of Tibetan Sheep
278 (*Ovis aries*) reflect animal age and nutritional requirement. *Frontiers in Veterinary Science*. 2020;7.

279 14. Saleem F, Bouatra S, Guo AC, Psychogios N, Mandal R, Dunn SM, et al. The bovine ruminal fluid
280 metabolome. *Metabolomics*. 2013;9 2:360-78.

281 15. Artegoitia VM, Foote AP, Lewis RM and Freetly HC. Rumen fluid metabolomics analysis associated with
282 feed efficiency on crossbred steers. *Scientific reports*. 2017;7 1:1-14.

283 16. De Almeida RTR, Do Prado RM, Porto C, Dos Santos GT, Huws SA and Pilau EJ. Exploring the rumen
284 fluid metabolome using liquid chromatography-high-resolution mass spectrometry and Molecular
285 Networking. *Scientific reports*. 2018;8 1:1-8.

286 17. Sun H-Z, Wang D-M, Wang B, Wang J-K, Liu H-Y, Guan LL, et al. Metabolomics of four biofluids from
287 dairy cows: potential biomarkers for milk production and quality. *Journal of proteome research*. 2015;14
288 2:1287-98.

289 18. Pahalagedara ASNW, Flint S, Palmer J, Subbaraj A, Brightwell G, Gupta TB. Antimicrobial Activity of
290 Soil Clostridium Enriched Conditioned Media Against *Bacillus mycoides*, *Bacillus cereus*, and
291 *Pseudomonas aeruginosa*. *Frontiers in Microbiology*. 2020;11.

292 19. Su M, Subbaraj AK, Fraser K, Qi X, Jia H, Chen W, et al. Lipidomics of Brain Tissues in Rats Fed Human
293 Milk from Chinese Mothers or Commercial Infant Formula. *Metabolites*. 2019;9 11:253.

294 20. Subbaraj AK, Huege J, Fraser K, Cao M, Rasmussen S, Faville M, et al. A large-scale metabolomics study
295 to harness chemical diversity and explore biochemical mechanisms in ryegrass. *Communications biology*.
296 2019;2 1:1-17.

297 21. Fraser K, Harrison SJ, Lane GA, Otter DE, Hemar Y, Quek S-Y, et al. Non-targeted analysis of tea by
298 hydrophilic interaction liquid chromatography and high resolution mass spectrometry. *Food chemistry*.
299 2012;134 3:1616-23.

300 22. Fraser K, Lane GA, Otter DE, Hemar Y, Quek S-Y, Harrison SJ, et al. Analysis of metabolic markers of
301 tea origin by UHPLC and high resolution mass spectrometry. *Food Research International*. 2013;53
302 2:827-35.

303 23. Holman JD, Tabb DL and Mallick P. Employing ProteoWizard to convert raw mass spectrometry data.
304 Current protocols in bioinformatics. 2014;46 1:13.24. 1-13.24. 9.

305 24. Forsberg EM, Huan T, Rinehart D, Benton HP, Warth B, Hilmers B, et al. Data processing, multi-omic
306 pathway mapping, and metabolite activity analysis using XCMS Online. *Nature protocols*. 2018;13 4:633.

307 25. Smith CA, Want EJ, O'Maille G, Abagyan R and Siuzdak G. XCMS: processing mass spectrometry data
308 for metabolite profiling using nonlinear peak alignment, matching, and identification. *Analytical
309 chemistry*. 2006;78 3:779-87.

310 26. Dunn WB, Wilson ID, Nicholls AW and Broadhurst D. The importance of experimental design and QC
311 samples in large-scale and MS-driven untargeted metabolomic studies of humans. *Bioanalysis*. 2012;4
312 18:2249-64.

313 27. Parsons HM, Ekman DR, Collette TW and Viant MR. Spectral relative standard deviation: a practical
314 benchmark in metabolomics. *Analyst*. 2009;134 3:478-85.

315 28. Cao M, Fraser K, Jones C, Stewart A, Lyons T, Faville M, et al. Untargeted metabotyping *Lolium perenne*
316 reveals population-level variation in plant flavonoids and alkaloids. *Frontiers in plant science*.
317 2017;8:133.

318 29. Wishart DS, Feunang YD, Marcu A, Guo AC, Liang K, Vázquez-Fresno R, et al. HMDB 4.0: the human
319 metabolome database for 2018. *Nucleic acids research*. 2018;46 D1:D608-D17.

320 30. Fahy E, Sud M, Cotter D and Subramaniam S. LIPID MAPS online tools for lipid research. *Nucleic acids*
321 *research*. 2007;35 suppl_2:W606-W12.

322 31. Guijas C, Montenegro-Burke JR, Domingo-Almenara X, Palermo A, Warth B, Hermann G, et al.
323 METLIN: a technology platform for identifying knowns and unknowns. *Analytical chemistry*. 2018;90
324 5:3156-64.

325 32. Foroutan A, Fitzsimmons C, Mandal M, et al. The Bovine Metabolome. *Metabolites*. 2020;5 10:E233.

326 33. Wheeler B, Torchiano M and Torchiano M. Package ‘lmPerm’. R package version, 2.1. 0. 2016.

327 34. Benjamini Y and Hochberg Y. Controlling the false discovery rate: a practical and powerful approach to
328 multiple testing. *Journal of the Royal statistical society: series B (Methodological)*. 1995;57 1:289-300.

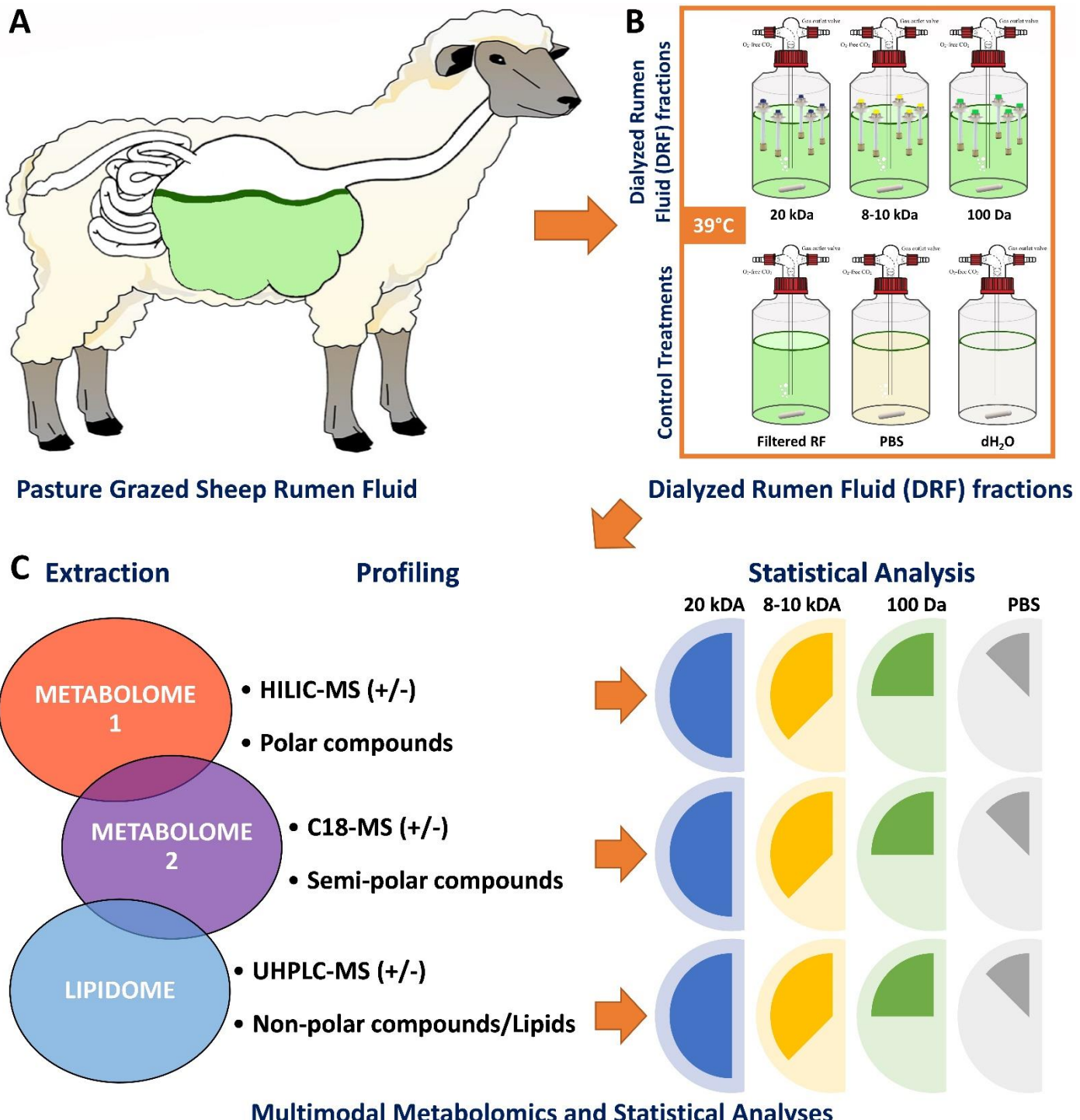
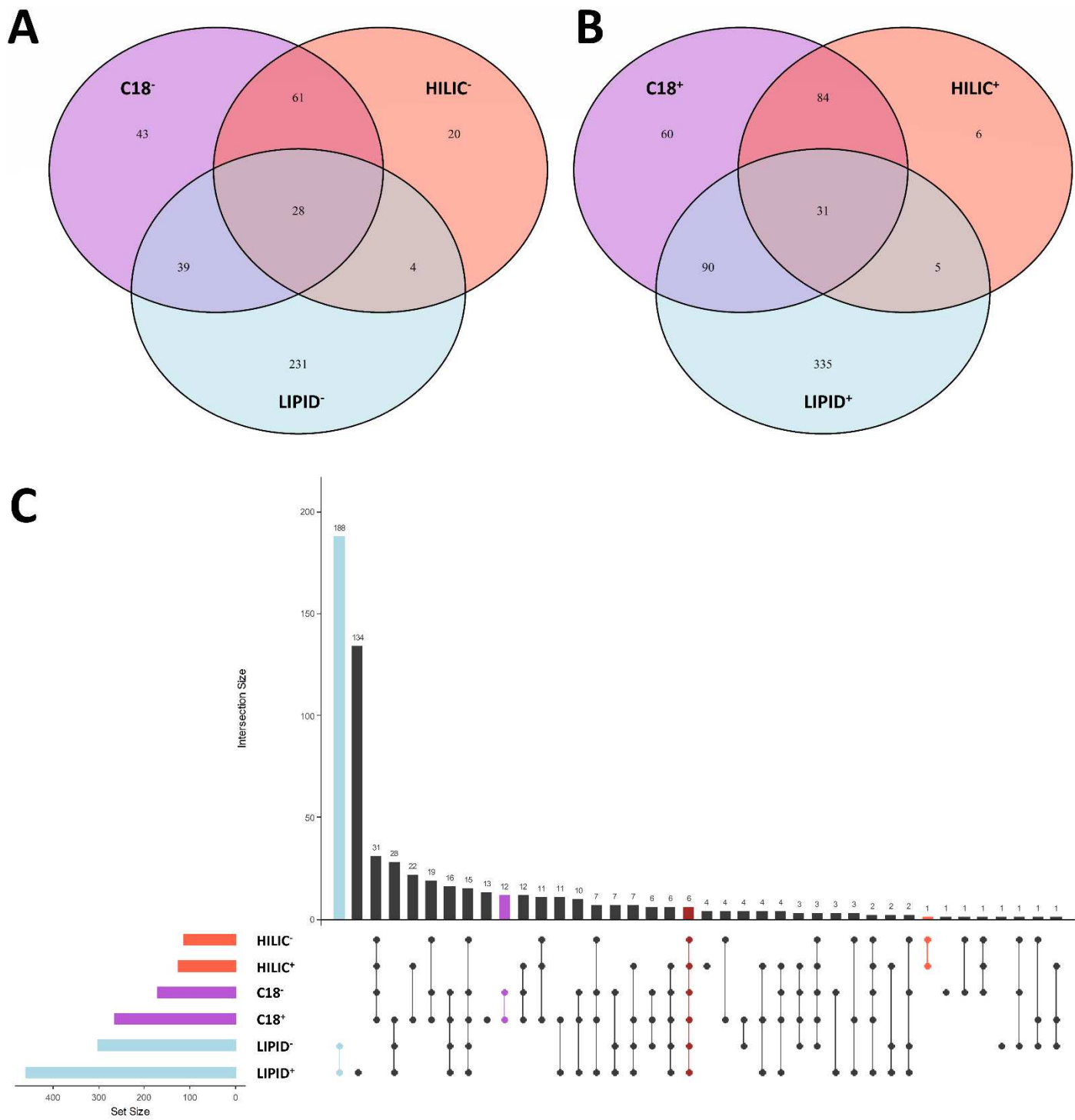


Figure 1. Overview of the experimental design and multimodal metabolomics workflow. (A) New Zealand pasture-fed sheep used for this study. **(B)** Dialyzed rumen fluid (DRF) fractions were obtained under anaerobic rumen conditions (39°C and CO₂) using dialysis systems at three molecular weight cut-offs. **(C)** Schematic of a multimodal metabolomics workflow and statistical analyses used to process data integrated from multiple analytical approaches.



335
336 **Figure 2. Unique and mutual peaks identified across all metabolomics streams.** Venn diagrams compiling
337 the Polar (HILIC), semi-polar (C18) and lipids (LIPID) molecular features determined from all DRF fractions
338 for the negative (A) and positive (B) streams. UpsetR barchart analysis (C) showing the presence and numbers
339 of quantified molecular features determined for different metabolomics streams (i.e. HILIC (orange), C18
340 (purple) and LIPID (blue)). Connected dots display shared molecular features between or among metabolomics
341 streams, and the total number of features in a particular metabolomics stream is shown in the set size. Coloured
342 connected dots indicate the molecular features identified in both the negative (-) and positive (+) extractions
343 of a metabolomics stream.